Industrial Engineering Journal
ISSN: 0970-2555
Volume : 54, Issue 1, No.4, January : 2025

COMPARATIVE ANALYSIS OF STATE VARIABLE AND ENERGY MAXIMIZATION APPROACHES FOR ENERGY MANAGEMENT IN HYBRID ENERFGY SYSTEMS FOR ELECTRIC VEHICLES

Neeraj Kumar Bahuguna, Department of Electrical Engineering, College of Technology, G.B. Pant University of Agriculture & Technology, Pantnagar. Uttarakhand, India.
Rajiv Singh, Associate Professor Department of Electrical Engineering, College of Technology, G. B. Pant University of Agriculture and Technology, Pantnagar, Uttarakhand, India.

ABSTRACT:
Energy management systems (EMS) are crucial for the EVs involving hybrid energy storage systems. EMS optimizes the performance of hybrid storage thereby enhancing the overall system efficiency and ensuring the durability of EV's energy storage system. Better energy management strategies are useful in maximizing the battery life by monitoring its state-of-charge (SOC) and temperature. Moreover, the EMS manages the power flow from the hybrid energy sources towards the power train and regulates the optimal energy usage based on the driving situations for achieving the maximum vehicle range. Managing multiple energy sources in hybrid storage systems pose serious challenges such as assessing the optimal power distribution and handling the energy consumption for maintaining the interfaces between energy systems for meeting the energy requirements of drive system and the accessories. In this paper two different EMS have been compared and analysed for a hybrid energy system containing PV array, Li-ion battery and a super-capacitor used for electric vehicles. The performance of external energy maximization strategy (EEMS) and state variable control strategy (SVCS) have been tested and evaluated in terms of their performance efficiency.
Keyword: Electric Vehicle, Energy management, PV array, Battery, SOC.

1. Introduction

Electrification of the modern transportation has reasonably grown world-wide due to its cleaner and less polluting character. The EV propulsion systems have largely use different types of batteries such as Lead acid, Li-ion and Sodium Sulphide for powering the electro-mechanical drive trains. However, to obtain enhanced reliability and better torque characteristics of the drive train hybrid energy sources are being used as alternatives for powering the EV drive train. The use of hybrid energy systems involving a PV panel, Li-ion battery and a supercapacitor is now days being explored for use in the EVs. The hybrid approach involves effective energy management strategies for optimal allocation of power amongst the different sources depending on the drive train requirements and their operational boundaries thereby minimizing the impact on the life cycle of hybrid system. This paper mainly focusses on two different EMS known as state variable (SVCS) and energy maximization (EEMS) approach for energy management of hybrid energy system for EVs[1]. A comparative analysis of these two strategies have been performed for a hybrid system involving a PV array a Li-ion battery and a super-capacitor for driving the EV motor. The analysis involves a comparison of the overall system efficiency for these two energy management strategies.

The paper's primary contribution lies in providing performance analysis and comparative analysis of SVSC and EEMS strategies for EVs comprising a PV array, Li-ion battery and a Super-capacitor. This evaluation considers their impact on overall efficiency and system lifecycle. This paper organized as follows: introduction is presented in section 1 followed by review of literature about different EMS used in EVs and their simulation-based analysis. Material and method are presented in section 3 describing the mathematical modelling of each component used in this strategy. Result and discussions are presented in section 4. Conclusion of the research are presented in section 5 and finally the references are presented.

2. Literature Review

This section presents the research previously conducted in the field of EMS. Key insights and important findings from these studies have been emphasized through a review of the literature presented below:

Snoussi et. al. (2018) explored the challenges in developing fuel cell hybrid electric vehicles (FCHEVs), focusing on power sources, EMS, power electronics configuration, and control techniques. The study emphasized optimizing the size of hybrid energy storage systems, for achieving better efficiency of FCHEVs. They proposed an optimal sizing method using a frequency-separation-based EMS, where filters were employed to the manage energy distribution, with one filter's frequency kept constant and the other dynamically updated. A multi-objective optimization algorithm, Multi-Objective Grey Wolf Optimization, was used to optimize both the energy management parameters and system mass. The study demonstrated the effectiveness of this approach in enhancing FCHEV performance and energy management.

Uebel et. al. (2018) introduced a novel approach combining Dynamic Programming (DP) and Pontryagin's Maximum Principle (PMP) for the online optimal control of hybrid electric vehicles (HEVs). This method accounted for various factors such as electric energy storage, engine state, gear selection, kinetic energy, and travel time, and was demonstrated using a parallel HEV. Compared to traditional DP methods, the proposed PMP-DP approach solved the optimal control problem over 100,000 times faster while maintaining solution quality close to the optimal. The study also evaluated its potential for real-time implementation, showing that it could be integrated into a vehicle control unit, particularly for sampling intervals of 20 meters or more. The PMP-DP method showed promise for significantly improving the speed and efficiency of HEV energy management.

Wang et. al. (2020) explored the management strategy of hybrid energy storage systems (HESS) in EVs, emphasizing its importance for ensuring safety and efficiency in the electric drive system. They employed an Adaptive Model Predictive Control (AMPC) approach, starting with an improved continuous power-energy method to configure the HESS using equivalent-circuit models for both the battery and supercapacitor. A novel predictive model was developed for a semi-active topology considering the DC load, which helped the AMPC handle the non-linearity and time-varying nature of HESS. The method was validated through three driving load cycle tests, showing that AMPC significantly outperformed other control methods, reducing the battery's peak current by 24.4%, total energy loss by 6.4%, Ah throughput by 16.2%, and root mean square of battery current by 29.8%.

Yu et. al. (2021) addressed the challenges of hybrid energy storage systems (HESS) combining lithium-ion batteries and supercapacitors, aimed at overcoming the limitations of battery-only storage in electric vehicles. Key issues such as high costs, low power density, and short cycle life have hindered the widespread adoption of electric vehicles. To address these, the study introduces a bi-level multi-objective design and control framework, using a non-dominated sorting genetic algorithm-II and fuzzy logic control. This framework optimizes both the size of the HESS and its real-time power management system, offering a more integrated and efficient solution.

3. Material and methods:

Figure 1 below depicts the block diagram representation of the simulated hybrid energy system driving a BLDC EV drive train. The mathematical models of each component is also presented in the sections below:

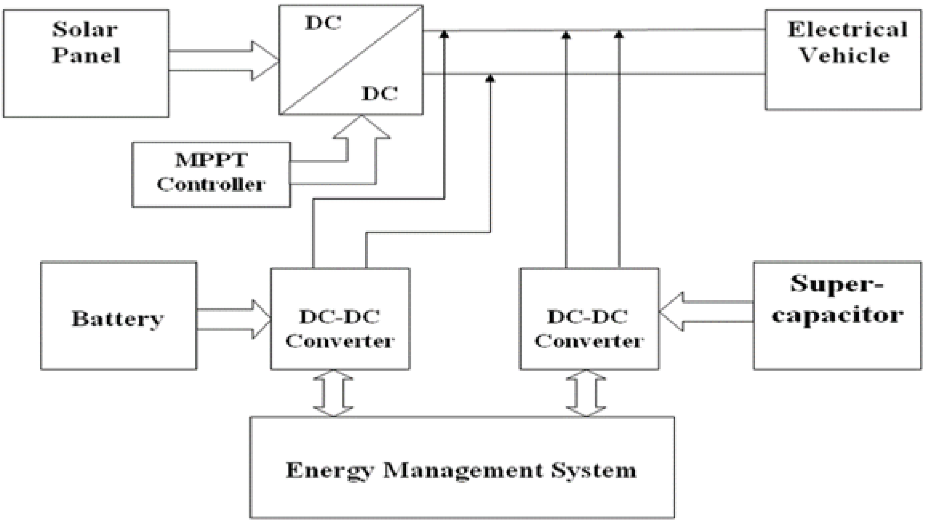

Fig. 1 Block diagram of hybrid energy system.

3.1 PV array

Fig. 2 depicts the equivalent circuit diagram of PV cell which is used for modelling the PV array. The mathematical model is represented by a series of equations (1)-(4) and the array design specifications are presented in Table 1.

Module Photo current is described by the equation 1

$$I_{photon} = [I_{SC} + k_I(T - 298)] \times \frac{I_r}{1000} \tag{1}$$

Where, I_{photon} is photo current (A); I_{SC} is short circuit current (A); k_I is short circuit current of cell at 25°C and 1000 W/m^2 and T is operating temperature (k); I_r is solar irradiation (W/m^2).

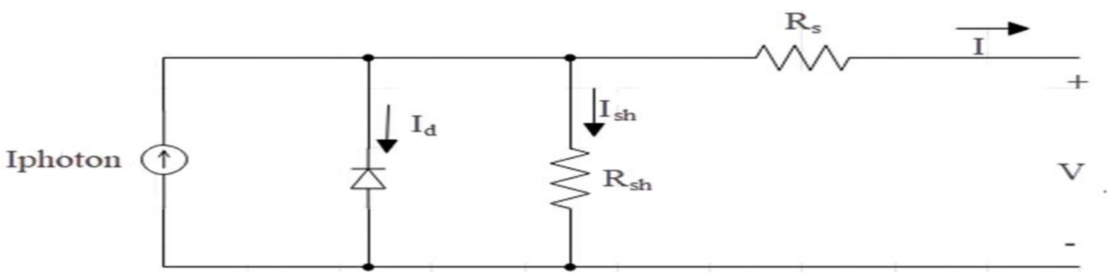

Fig. 2 Equivalent circuit of PV cell

Module reverse saturation current I_{rs} is described by equation (2))

$$I_{rs} = \frac{I_{sc}}{[exp(\frac{qV_{oc}}{N_s K n T}) - 1]} \tag{2}$$

Where, q represents electron charge which is 1.6× 10^{-19}C; V_{oc} is open circuit voltage (V); N_s is the number of cell connected in series; n is ideality factor of the diode; k is Boltzmann's constant which is 1.38 × 10^{-23}J/k [2].

The diode I-V characteristic is defined by equation (3) and (4)

$$I_{diode} = I_o \left[exp\left(\frac{V_d}{V_T}\right) - 1\right] \tag{3}$$

Where, I_{diode} is diode current; I_o is diode saturation current; V_d is diode voltage (V); V_T is terminal voltage (V).

$$V_T = \frac{kT}{q} \times n \times N_{cell} \tag{4}$$

Where, N_{cell} is Number of cells connected in series in a module

The table 1 shows the design specification of PV array:

Table 1: Design specification of PV array[2]

Design specification	Values
Open circuit voltage (V)	44.7
Short circuit current (A)	8.78
Temperature coefficient of V_{oc} (%/°c)	-0.4051
Temperature coefficient of I_{sc} (%/°c)	0.075604
Voltage at maximum power point (V)	36.1
Current at maximum power point (A)	8.31

3.2 Supercapacitor Model

The equivalent circuit model for Super-capacitor (SC) is depicted in Fig. 3 and the modeling parameters are given in Table 2. SC is an energy storage device which offers high-power density, making it useful in specific applications such as EVs. Unlike batteries, SCs have a lower energy density but offer higher power density[2],[3].

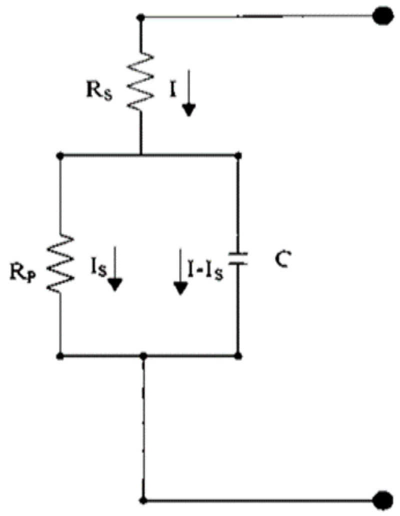

Fig. 3: Electrical equivalent circuit of SC

The SCs output voltage is expressed in equation 5

$$V_{Supercap} = \frac{N_s Q_T d}{N_p N_e \varepsilon \varepsilon_0} + \frac{2 N_e N_s RT}{F} Sinh^{-1}\left(\frac{Q_T}{N_p N_e^{\,2} Ai \sqrt{8RT\varepsilon\varepsilon_0 C}} \right) \tag{5}$$

Where, A_i is Interfacial area between electrodes and electrolyte (m^2), I_{sc} is SC current (A), V_{sc} = SC voltage (V), C_T is Total capacitance (F), R_{sc} is Total resistance (ohms), C is Molar concentration (mol/m^3), R is Molecular radius (m), F is Faraday constant, N_e is number of layers of electrodes, N_A is Avogadro constant, N_p is number of parallel SC, N_s is number of series SC, Q_T is Electric charge (C), R is Ideal gas constant, d is Molecular radius, T is Operating temperature (K), E is Permittivity of material and ε_0 is Permittivity of free space[2],[3].

Table 2 shows the design specification of SC:

Table 2: Design specification of SC

Design specification	Values
Rated capacitance (F)	15.6
Equivalent DC series resistance(ohm)	0.150
Rated voltage (V)	290.6
Number of series capacitance	2
Number of parallel capacitances	5

3.3 Li-ion Battery Model

Li-ion battery is modelled on the basis of equivalent circuit depicted in fig. 4. The charging and discharging behavior of the battery are modelled as per equation (6) and (7) and the design parameters given in Table 3.

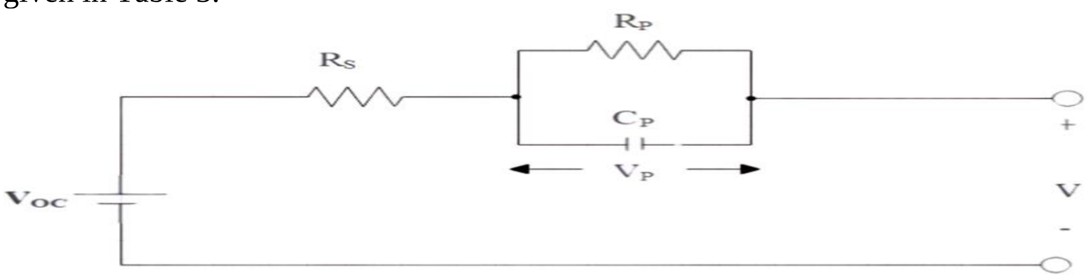

Fig. 4: Electrical circuit model of Li-ion battery

For charge model (I^0>0):

$$F_1(it, I^0, I) = E_0 - K\frac{Q}{Q-it}I^0 - K\frac{Q}{Q-it}it + A.Exp(-B.it) \tag{6}$$

For discharge model (I^0<0):

$$F_1(it, I^0, I) = E_0 - K\frac{Q}{0.1Q+it}I^0 - K\frac{Q}{Q-it}it + A.Exp(-B.it) \tag{7}$$

Where, E_0 is constant voltage in V, Exp(s) is exponential zone dynamics in V, Sel(s) is battery mode, Sel(s) is 0 (during battery discharge), Sel(s) is 1 (during battery charging), K is polarization constant in V/Ah, I^0 is low-frequency current dynamics in A, I is battery current in A, it is extracted capacity in Ah, Q is maximum battery capacity in Ah, A is exponential voltage in V and B is exponential capacity in Ah^{-1}[4].

Table 3: Parameter specification of Li-ion battery[4].

Design specification	Values
Nominal voltage(V)	48
Rated capacity (Ah)	343.75
Initial SoC(%)	65
Battery response time(s)	1
Maximum capacity(Ah)	300
Cut off voltage(V)	36

3.4 Power Converters

The power converters used in this work are modelled on the basis of equivalent circuits depicted in figs. 5 and 6 representing a buck and a boost converter respectively. The converters are important in a drive system as they are used for controlling the flow of energy from the battery and other energy sources in a hybrid energy system[3],[4].

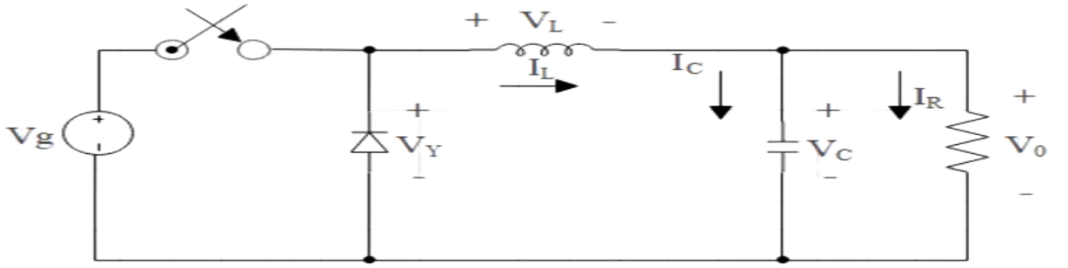

Fig. 5: Schematic diagram of buck converter

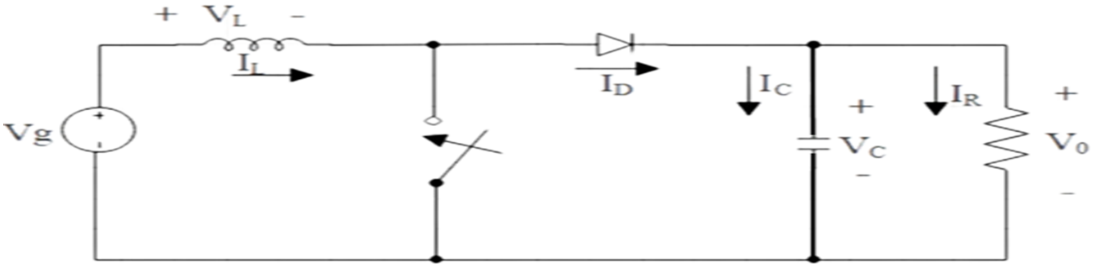

Fig. 6: Schematic diagram of boost converter[4].

3.5 Modeling of Electric Drive

In this work the EV drive train is represented by a brushless DC(BLDC) motor having back emf characteristics of Trapezoidal shape. The Trapezoidal shape of the back emf indicates that the mutual inductance between the stator and rotor follows trapezoidal curve for one rotation of the rotor[2],[3],[4]. The motor's model has been created by using three phase a,b,c variables instead of on the basis of conventional two phase d-q variables. The model considers certain assumptions such as neglecting magnetic circuit saturation, assuming equal and constant stator resistance, self-inductance, and mutual inductance for all phases, disregarding hysteresis and eddy current losses etc. for the model. The Phase voltage equations representing BLDC motor is given in equation 8 to 10:

$$V_a = Ri_a + (L - M)\frac{di_a}{dt} + E_a \tag{8}$$

$$V_b = Ri_b + (L - M)\frac{di_b}{dt} + E_b \tag{9}$$

$$V_c = Ri_c + (L - M)\frac{di_c}{dt} + E_c \tag{10}$$

Torque equations are each phase of BLDC motor are given in equations (11)-(14):

$$T_a = K_t . i_a . f.(\phi_e) \tag{11}$$

$$T_b = K_t . i_b . f.\left(\phi_e - \frac{2\pi}{3}\right) \tag{12}$$

$$T_c = K_t . i_c . f.\left(\phi_e - \frac{4\pi}{3}\right) \tag{13}$$

The electromagnetic torque is

$$T = T_a + T_b + T_c \tag{14}$$

3.6 State Variable Control Strategy

A state variable control strategy uses a set of predefined states defining the system operation and controls the transition of system operation amongst these states for optimally managing the energy flow amongst the different sources [2],[5], [6]. Each state denotes a particular operating mode or condition for the hybrid energy system and the transitions represent the reaction of system towards changes in the conditions such as load demands and the available power from the different energy sources.

Figures 7 and 8 respectively represents the functioning of EMS operating State variable control strategy during the functioning of PV array and battery respectively.

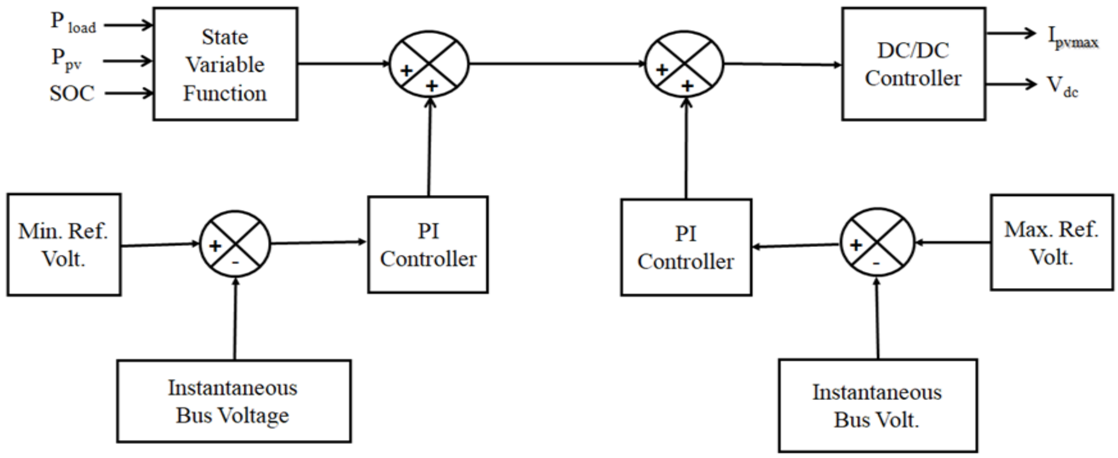

Fig. 7: State variable control strategy during PV array operation.

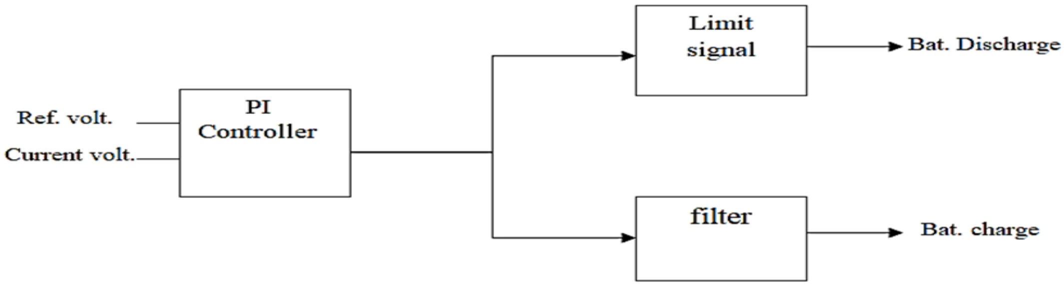

Fig. 8: State variable control strategy during battery operation.

The transition of system states depends on the parameters such as load demands, PV array generation and also the charge content of battery and supercapacitor. When the load demand is low and PV array generation is abundant the system state will shift to *"battery charging*" mode diverting the excess energy generated into the battery for charging. However, when the load demand is high, or when the PV array generation is insufficient the control strategy leads to the transition of state to *"battery discharging"* mode in which the battery delivers the stored energy to fulfill the load requirements. Also, for short requirements of high power the state transition may also vary from *"discharging super capacitor"* to *"charging supercapacitor"* depending on the load power requirements.

The proposed state variable control strategy used eight states for defining the system operation as illustrated in Table 4 and the reference value of system parameters used in the control algorithms are given in Table 5. The output power from the PV array is determined on the basis of battery SOC and the load power requirements (P_{load})[2],[3],[7].

Industrial Engineering Journal
ISSN: 0970-2555
Volume : 54, Issue 1, No.4, January : 2025

Table 4: States of state variable control strategy.

If SOC Normal & $P_{load} > P_{pvmin}$	State = 1	$P_{pv} < P_{pvmin}$
If SOC Normal & $P_{load} > P_{pvmax}$	State = 2	$P_{pv} > P_{pvopt}$
If SOC High & $P_{load} \geq P_{pvmax}$	State = 3	$P_{pv} = P_{pvmax}$
If SOC Normal & $P_{load} < P_{pvopt}$	State = 4	$P_{pv} = P_{pvmax}$
If SOC Normal & $P_{load} \in [P_{pvopt}, P_{pvmax}]$	State = 5	$P_{pv} = P_{pvopt}$
If SOC Normal & $P_{load} \geq P_{pvmax}$	State = 6	$P_{pv} = P_{pvmax}$
If SOC Low & $P_{load} < P_{pvmax}$	State = 7	$P_{pv} = P_{load}$
If SOC Low & $P_{load} \geq P_{pvmax}$	State = 8	$P_{pv} = P_{pvmax}$

Table 5: Reference values of variables used in EMS approaches

S.No.	System State	Reference Value
1.	SOC_{min}	60
2.	SOC_{nom1}	85
3.	SOC_{nom2}	60.1
4.	$SOC_{max.}$	90
5.	P_{pvmin}	50 Watt
6.	P_{pvmax}	540 W
7.	$P_{battmax}$	3400 W

The control module manages the overall system performance by using the state variable control approach and considering the state of charge present in battery and the supercapacitor both including the operational limits of the system parameters. The battery and the supercapacitor are charged and discharged on the basis of the system conditions as mentioned above.

3.7 External Energy Maximization Strategy (EEMS)

The description of EEMS for hybrid energy systems comprising a solar PV array, a Li-ion battery and a Supercapacitor and external source for EVs is presented in this section. Its main goal is to maximize the use of external energy sources, such as grid electricity, to lessen dependence on internal energy storage components and enhance overall efficiency [8]. The EEMS continuously tracks the availability and cost of external energy from the grid, taking into account factors such as electricity prices, grid stability, and user preferences. It also estimates the energy demand of the EV based on driving patterns, route planning, and user requirements [5],[6],[7]. The strategy uses optimization algorithms for determining the best allocation amongst the energy sources, for deciding the amount of energy to be drawn from the PV array, battery, SC, and external source for meeting the instantaneous energy demands while minimizing the costs for maximizing the use of external energy [9].

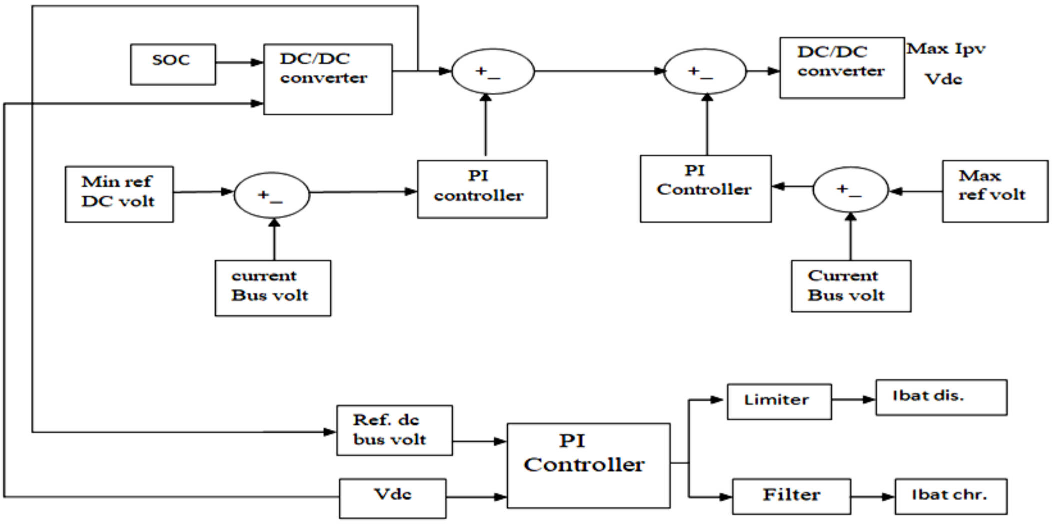

Fig. 9: Block diagram of EEMS.

The primary objective of EEMS is to maximize the utilization of external energy while minimizing the costs. Therefore, the objective function for this optimization problem is defined according to equation (15).

$$F_{\max} = \sum_{t-1}^{T} E_{ext}(t) - \sum_{t-1}^{T} C_{\text{int}}(t) \tag{15}$$

Where,

$F_{\max}$ = objective function to maximize external energy usage.
$E_{\text{ext}}(t)$ = external energy consumed at time t.
$C_{\text{int}}(t)$ = cost or penalty associated with internal energy usage.
The energy balance equation is given by equation (16)

$$E_{load}(t) = E_{PV}(t) + E_{bat}(t) + E_{sc}(t) + E_{ext}(t) \tag{16}$$

Where,

$E_{\text{load}}(t)$ = Energy demand of the EV load at time t.
$E_{\text{PV}}(t)$ = Energy harvested from the PV array.
$E_{\text{bat}}(t)$ = Energy flow to/from the battery.
$E_{\text{sc}}(t)$ = Energy flow to/from the SC.
$E_{\text{ext}}(t)$ = Energy obtained from the external source.

4. Results and Discussion

The results obtained from the simulation-based study conducted for the two EMS i.e. SVCS and EEMS and their explanation are presented in this section. Figure 10 depicts the Li-ion battery current, its voltage and SOC separately during the different conditions of load requirements.

It is evident from the graphs that the battery is inactive from 0 to 3.5 seconds, resulting in a battery current of 0 amperes. During this period, power is provided by the PV array and SC. After 3.5 seconds, as the load power rises from 1342 to 1354 watts, the battery begins to operate, and the current value gradually increases, as shown in the battery current curve. At the same time, the battery voltage drops from 52.5 V to 51.5 V. The initial SOC of the battery is 65%, which decreases to 64.3% during the 0 to 50 seconds interval.

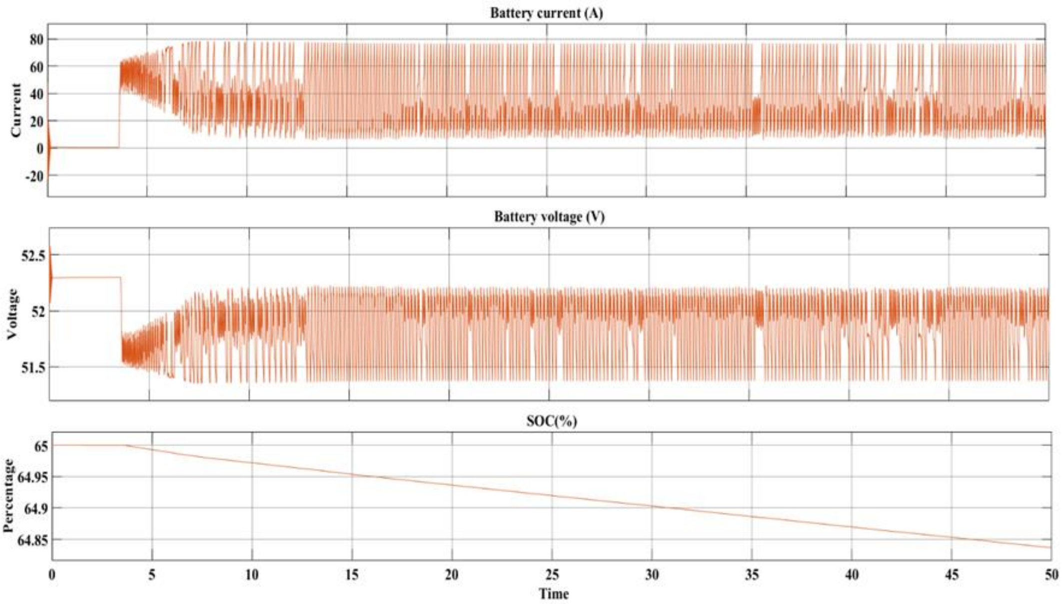

Fig. 10: Battery current, voltage, and SOC curve of state variable strategy.

Figure 11 illustrates the behavior of the SC following its initial discharge, with both the current and voltage graphs displaying small but rapid oscillations. This pattern indicates that the SC is frequently activating and deactivating to stabilize quick fluctuations in the power demand, which is the typical function of SCs in EMS. The graph shows that the SC voltage decreases from 269 V to 267.8 V, while the current increases from 2 A to 10 A during the time interval of 0 to 3.5 seconds. From 3.5 seconds to 50 seconds, the SC current fluctuates between -5 and 5 A, and the voltage ranges from 269 V to 271V.

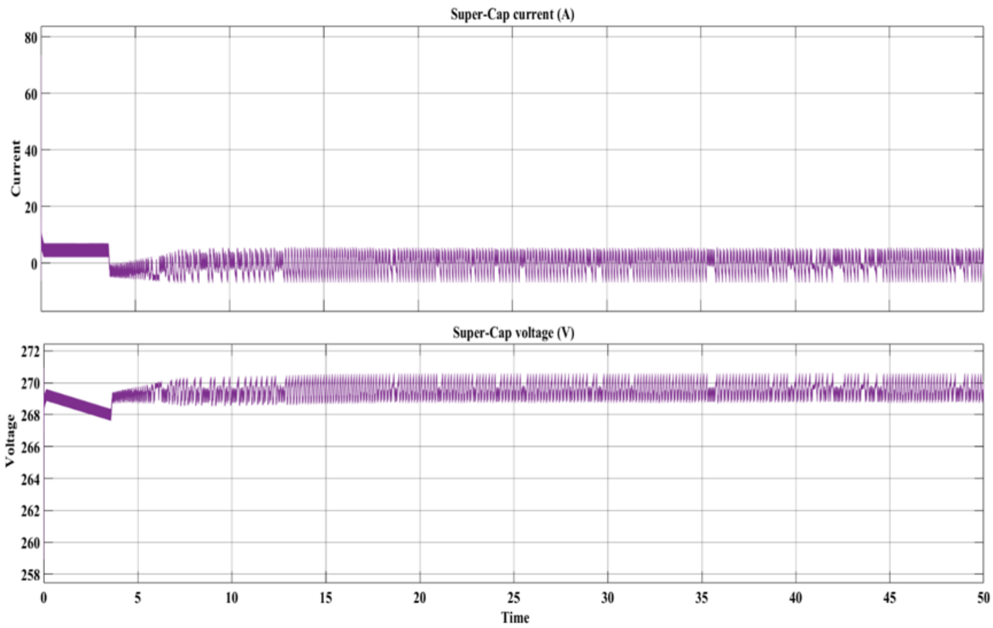

Fig. 11: SC current, voltage curve of state variable control strategy

Figure 12 shows that the management of power coming from PV array, battery and Supercapacitor flowing towards the load is effectively managed using SVCS for a time duration of 50 Seconds.

According to the rules of the SVCS outlined in Table 7, when the battery SOC is high and the load power requirement exceeds the minimum value of PV power (P_{pvmin})), then the load power switches on the battery. This condition is fulfilled by the power curve depicted in Figure 12. At 0.5 seconds, the SOC is at 65%, the PV power is 12 watts, and the load power requirement is 670 watts, which exceeds the minimum PV power. At 4 seconds, the graph also meets the criteria for State 2, where the SOC remains at 65%, and the load power is 1770 watts, surpassing the maximum PV power. Here, the PV power of 450 watts exceeds the operating power of the PV array, which is 250 watts. Additionally, all other rules of the SVCS are adhered to, with the power output from the PV array, battery, and SC being regulated accordingly. The power output from the PV array, battery, and SC exhibits variability, with the SC responding frequently to immediate fluctuations. Hence, the result curves satisfy the characteristic of SVCS, where the system transitions between different operational modes (charging and discharging) based on load requirements and the status of the energy sources.

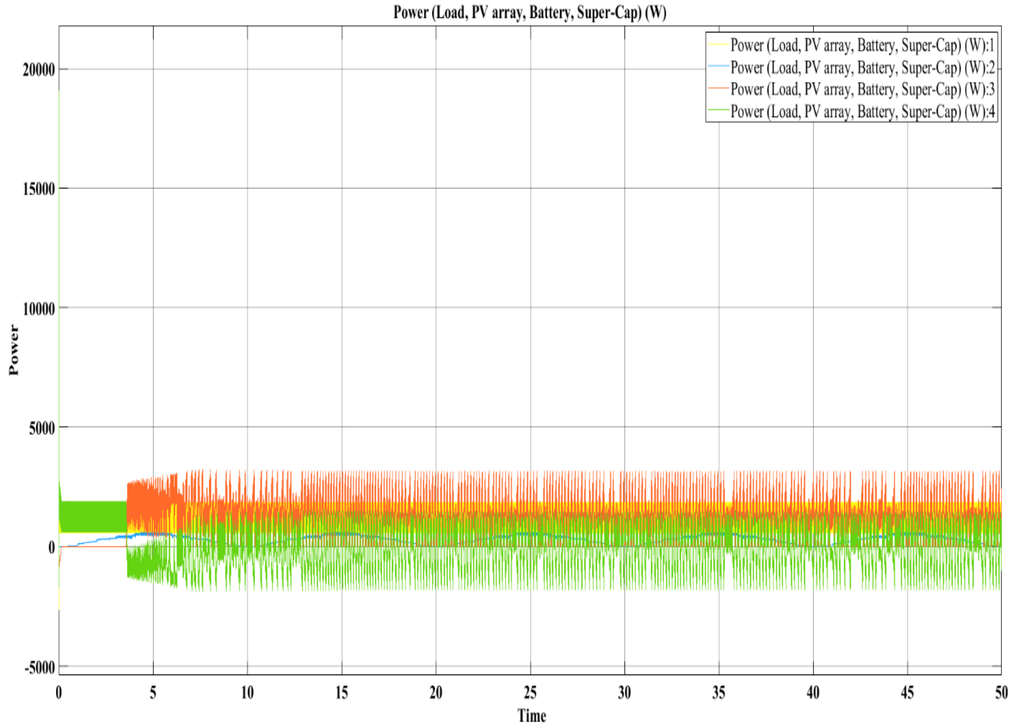

Fig. 12: Power curve of load, PV array, battery, SC in SVCS

Overall, the SVCS depicted in these graphs is defined by their specific operational states, demonstrating the transitions to various power levels. This approach efficiently manages the interactions amongst the PV array, battery, and SC to ensure a stable power supply to the load. The role of the SC for quick responses and the battery for longer-term energy balance is clear, and the fluctuations in the converter input voltages reflect active management of both energy generation and storage components.

Fig. 13 shows the operating conditions of battery during the implementation of EEMS. It can be observed that the Battery current exhibits a notable initial spike and then exhibits consistent oscillations, which are indicative of the battery cycling between charging and discharging in response to the control strategy. The battery voltage remains relatively steady with minor fluctuations, reflecting a balance between the battery's charge and discharge processes. The variation of battery current is from 18 A to 60A. Initially the battery current is zero after the battery operation the current increases and shows the continuous variation for duration of 50 second. SOC exhibits a gradual and linear decline over the 50 seconds, indicating a controlled discharge rate, likely aimed at maximizing the use of external energy while maintaining battery health. In the third section of the graph, the SOC starts at 65% during the time period from 0 to 4 seconds, and it decreases to 64.85% by the 50th second during discharging.

Industrial Engineering Journal
ISSN: 0970-2555
Volume : 54, Issue 1, No.4, January : 2025

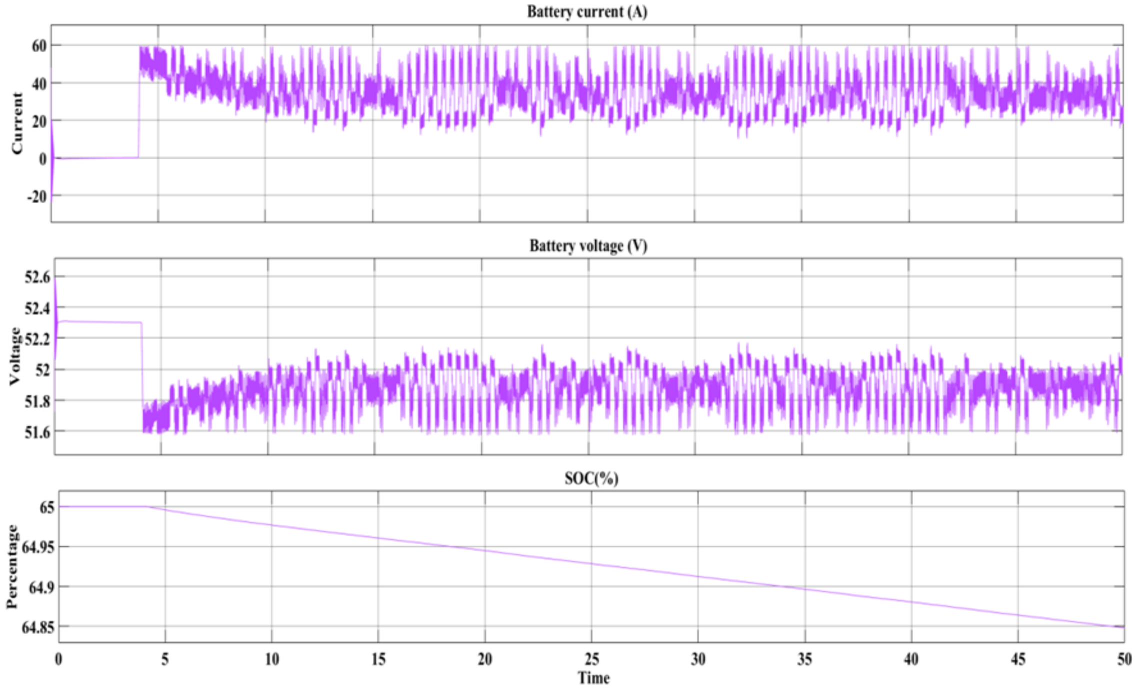

Fig. 13: Battery current, voltage, and SOC curve of EEMS

The Fig. 14 shows the converter voltage and current graphs. SC current experiences a drop initially, stabilizing with smaller fluctuations throughout the rest of the period, showing its role in short-term energy storage and release. The voltage of the SC decreases slightly and then stabilizes, reflecting a maintenance of balance between charge and discharge to support system voltage stability.

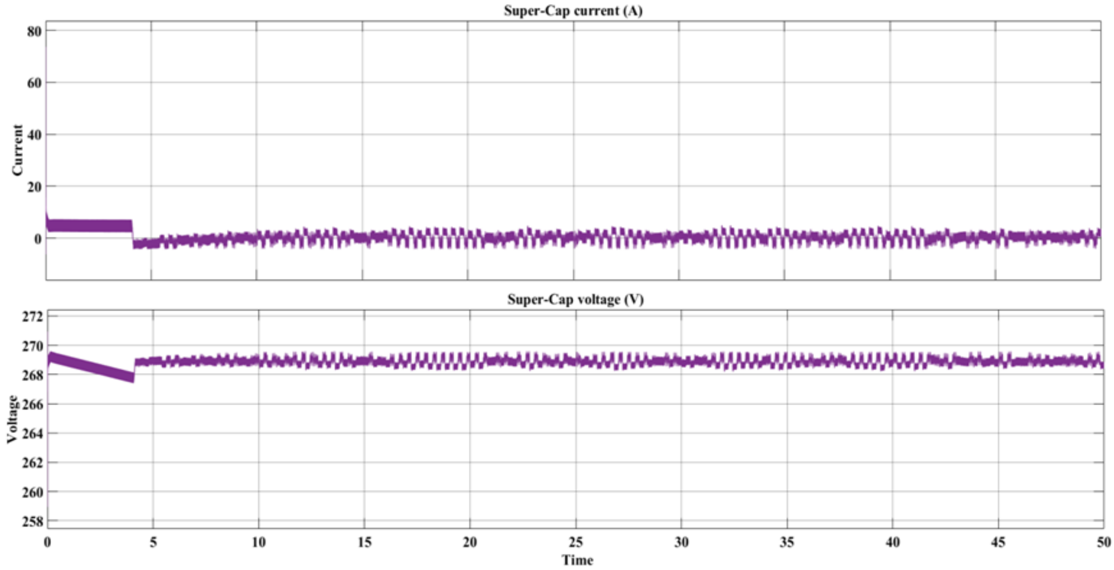

Fig. 14: SC current, voltage curve of EEMS.

The Fig. 15 shows the power shared among the load, PV array, battery, and SC. Initially, there is a stabilization period after a sharp rise, due to the system engaging to meet the demand. The PV array shows a consistent contribution, with less variability than the other sources, which may be due to the maximization strategy prioritizing the use of external energy sources. The power from the battery and SC shows some oscillations, suggesting they are compensating for transient imbalances between load demand and PV supply.

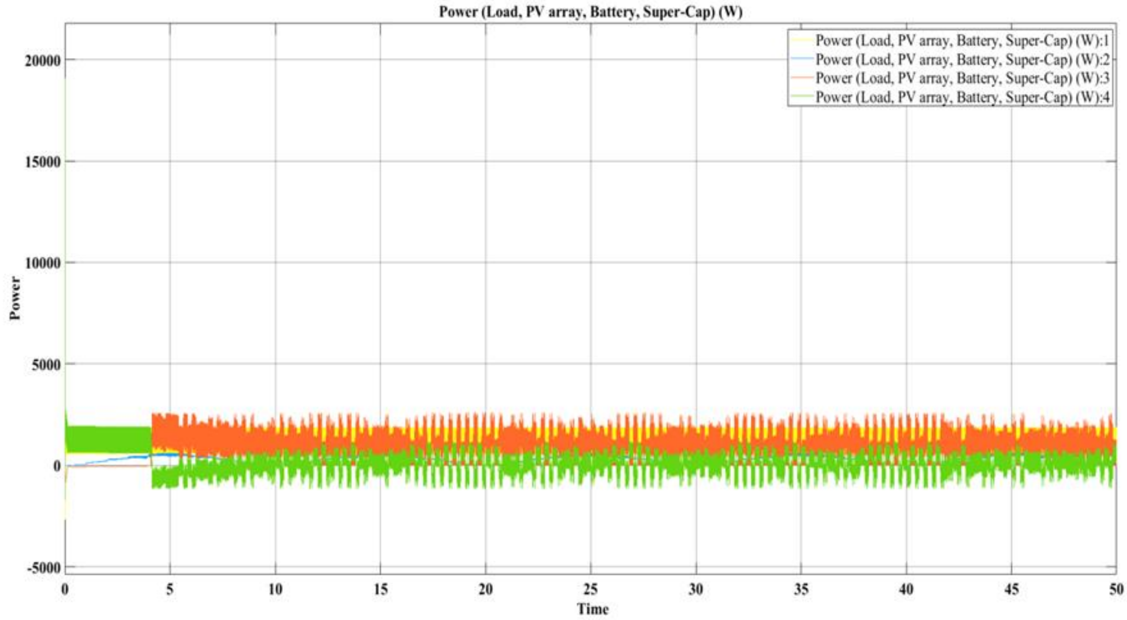

Fig. 15: Power curve of load, PV array, battery, SC in EEMS

The Fig. 12 and 15 illustrates a comparison of the load power among the SVC and EEM strategies. In the SVCS, the maximum load power is 1873 W and the EEM strategy it reaches 1854 W.

The table 6 shows the comparison of both the strategies according to different parameters. The overall efficiency of the system performance is computed by equation (17).

$$Efficiency = \frac{P_{load}}{P_{pv} + P_{battery} + P_{sup\,cap.}} \qquad (17)$$

Table 6: Comparative analysis of both strategies

Strategy	**SVC**	**EEMS**
Power Distribution	Distinct operational states, transitions between modes, variability in sources	Stabilization after initial rise, consistent PV array contribution, oscillations in battery and supercapacitor
Battery Metrics	SOC decreases linearly, managed discharge rate	Gradual decline, controlled discharge rate, maximizing external energy
Supercapacitor Metrics	Immediate discharge, frequent engagement, smoothing out rapid changes	Initial drop, stabilization with smaller fluctuations
Converter Input Voltages	Variability in PV array and battery converter input voltages	Waveform pattern, adjustments to maximize solar power
Overall Characteristics	Effective management of interactions, distinct states, stable power supply	Optimal use of external energy, balanced stability, managed component health
Efficiency	80.36%	81.52%

5. Conclusion

The study conducted a thorough analysis of EMS using SVCS and EEMS highlighting their benefits and drawbacks, systematically assessed through simulation. The analysis of these two EMS provides valuable insights into their respective strengths and weaknesses. Each strategy exhibited unique characteristics in responding to varying operating conditions, and this comparative study laid the foundation for informed discussions on the most effective strategies for specific contexts. The study highlighted the importance of considering factors such as system stability, component health, adaptability to fluctuations, and long-term sustainability when selecting an EMS.

6. References

[1**]** Dusmez, S. and Khaligh, A. 2014. A supervisory power-splitting approach for a new ultracapacitor-battery vehicle deploying two propulsion machines. *IEEE Trans. on Ind. Inf.,* 10(3):1960-1971.
[2] Neeraj Bahuguna Kumar, Singh Rajiv, (2024). Assessment of State Variable Control Approach for Energy Management of Hybrid Energy System for Electric Vehicles, Industrial Engineering Journal, 53 (3), pp. 49-59.
[3] Neeraj Bahuguna Kumar, Singh Rajiv, (2023). Simulation and critical evaluation of a two-wheeler EV system under varying aerodynamic and terrain conditions, Industrial Engineering Journal, 52 (1), pp. 46-55.
[4] Singh Rajiv (2023), Modelling of Lithium-Ion batteries with distinct chemistries using novel and advanced system identification-based data-driven approach, Industrial Engineering Journal, 52 (2), pp. 74-86.
[5] Ehsani, M., Rahman, K.M. and Toliyat, H.A., 1997. Propulsion system design of electric and hybrid vehicles. *IEEE Trans. on ind. Elect.*, *44*(1):19-27.
[6] Snoussi, J., Elghali, S. B., Benbouzid, M. and Mimouni, M. F. 2018. Optimal sizing of energy storage systems using frequency-separation-based energy management for fuel cell hybrid electric vehicles. *IEEE Trans. Veh. Tech.*, *67*(10):9337-9346.
[7] Uebel, S., Murgovski, N., Tempelhahn, C. and Baker, B. 2018. Optimal Energy Management and Velocity Control of Hybrid Electric Vehicles. *IEEE Trans. on Veh. Tech.*, *67*(1): 327-337.
[8] Wang, F., Mei, X., Rodriguez, J. and Kennel, R. 2020. Model predictive control for electrical drive systems-an overview. *CES Trans. on Elect. Mach. and Sys.*, *1*(3):219-230.
[9] Yu, H., Castelli-Dezza, F., Cheli, F., Tang, X., Hu, X. and Lin, X. 2021**.** Dimensioning and Power Management of Hybrid Energy Storage Systems for Electric Vehicles with Multiple Optimization Criteria. *IEEE Trans. on Power Elect.*, *36*(5):5545-5556.